Superharmonic Resonance of an Electrically Actuated Resonant Microsensor

Eihab M. Abdel-Rahman and Ali H. Nayfeh

Department of Engineering Science and Mechanics, MC 0219, Virginia Polytechnic Institute and State University, Blacksburg, Virginia 24061, USA, anayfeh@vt.edu

ABSTRACT

We investigate the response of a microbeam-based resonant sensor to a superharmonic electric actuation. The model incorporates the nonlinearities associated with moderately large displacements and electric forces. The method of multiple scales is used to obtain two first-order nonlinear ordinary-differential equations that describe the modulation of the amplitude and phase of the response and its stability.

We present typical microsensor frequency-response and force-response curves. The curves demonstrate the existence of multivalued solutions. These curves consist of three branches which meet at two saddle-node bifurcation points. The results provide an analytical tool to predict the microsensor response to superharmonic excitations, specifically the locations of sudden jumps and regions of hysteretic behavior, thereby enabling designers to safely use this frequency as a measurement signal.

Keywords: MEMS, resonant sensors, forced vibrations, superharmonic resonance.

1 INTRODUCTION

Electrically actuated microbeams are widely used as MEMS resonant sensors [1-9]. These devices employ the shift in the fundamental natural frequency of a microbeam due to an applied axial load to measure external factors, such as pressure, temperature, force, and acceleration.

Experimental [1], [2] and analytical works [2], [3] have shown that increasing the driving AC voltage leads to bending of the frequency-response curves to the right (hardening behavior) and generating hysteretic behavior near the primary-resonance frequency. Other experimental [4]–[6] and analytical studies [4], [6] of MEMS devices have shown both softening and hardening behavior, depending on the geometry and operating conditions of the device and the assumptions made in the model. These results show that the nonlinear behavior results from the interaction of various distinct phenomena; namely, the mechanical restoring force, which stiffens the microbeam (shifting the natural frequencies to higher values), and the electrostatic force, which softens the microbeam (shifting the natural frequencies to smaller values).

Recent research [7] has shown experimentally that using a superharmonic excitation of order-two to drive resonant microsensors increases the signal-to-crosstalk ratio as compared to driving the resonator at primary resonance. However, there is no analytical work in the literature on the superharmonic resonance of microsensors.

In a previous work [8], we introduced a nonlinear model for a clamped-clamped microbeam, which accounts for the static deflection due to the electrostatic force, moderately large displacements, and the nonlinearity produced by the electric forcing. We used the method of multiple scales to obtain an approximation of the response of the microbeam to primary resonance [9].

In this paper, we expand on that work and study the microbeam response to a superharmonic electric actuation. We model the microbeam as a distributed-parameter system. We apply the method of multiple scales to obtain an approximation of the microbeam response. We derive two equations that describe the modulation of the amplitudes and phases of periodic solutions and the stability of these solutions.

2 PROBLEM FORMULATION

We consider a microbeam actuated by an electric force composed of a DC component (polarization voltage) V_p and a superharmonic component $v(t) = F\cos(\Omega t)$. The DC component statically deflects the microbeam to a new equilibrium position, while the AC component actuates it around this equilibrium position. We write the nondimensional equation of motion governing the transverse deflection $w(x)$ of the microbeam under transverse electric forces as [8]

$$\ddot{w} + c\dot{w} + w^{iv} = \left[\alpha_1\Gamma(w,w) + N\right]w'' + \alpha_2\frac{\left(V_p + v(t)\right)^2}{\left(1-w\right)^2} \tag{1a}$$

$$w(0,t) = w(1,t) = 0,\ w'(0,t) = w'(1,t) = 0 \tag{1b}$$

where $\Gamma\left[f_1(x,t), f_2(x,t)\right] = \int_0^1 f_1' f_2' dx$, α_1, and $\alpha_2 V_p^2$ are nondimensional parameters, which are functions of the device specifications, N is the nondimensional applied axial load, and c is the nondimensional viscous

damping coefficient. The primes indicate derivatives with respect to x, the length of the microbeam, and the overdots indicate derivatives with respect to time t.

The microbeam deflection is composed of a static component $w_s(x)$ due to V_p^2, a forced component $\eta(x)$ due to $2V_p v(t)$, and a resonant component $u(x,t)$ due to $v(t)^2$; that is,

$$w(x,t) = w_s(x) + F\eta(x)\cos(\Omega t) + u(x,t) \tag{2}$$

where $w_s(x)$ is given by

$$w_s^{iv} = [\alpha_1 \Gamma(w_s, w_s) + N]\, w_s'' + \frac{\alpha_2 V_p^2}{(1 - w_s(x))^2} \tag{3a}$$

$$w_s = 0 \text{ and } w_s' = 0 \quad \text{at} \quad x = 0 \text{ and } x = 1 \tag{3b}$$

and $\eta(x)$ is given by

$$\eta^{iv} = [\alpha_1 \Gamma(w_s, w_s) + N]\, \eta'' + 2\alpha_1 \Gamma(w_s, \eta) w_s'' + \frac{2\alpha_2 V_p^2}{(1 - w_s(x))^2} + \frac{2\alpha_2 V_p^2}{(1 - w_s(x))^3}\eta + \Omega^2 \eta \tag{4a}$$

$$\eta = 0 \text{ and } \eta' = 0 \quad \text{at} \quad x = 0 \text{ and } x = 1 \tag{4b}$$

We order the harmonic forcing $v(t)$ at $O(u^{\frac{3}{2}})$ and damping c at $O(u^2)$ and solve the distributed-parameter problem arising from equations (1) directly using the method of multiple scales [10], [11] to determine a uniformly valid approximate solution. To describe the nearness of the excitation frequency Ω to one-half the natural frequency ω_n, we introduce the detuning parameter σ defined by $\Omega = \frac{1}{2}\omega_n + \sigma$. Carrying out the multiple scales analysis, we obtain the microbeam response, to the second approximation, to a superharmonic excitation of order-two as

$$w(x,t) = w_s(x) + F\cos(\Omega t)\eta(x) + a\cos(2\Omega t + \gamma)\phi_n(x) + \tfrac{1}{2}a^2\left[\cos(4\Omega t + 2\gamma)\psi_1(x) + \psi_2(x)\right] + \cdots \tag{5}$$

where $\phi_n(x)$ is the *nth* linear-undpamed mode shape of the microbeam around the deflected position $w_s(x)$, $\psi_1(x)$ and $\psi_1(x)$ are solutions of two boundary-value problems associated with the second-order perturbation problem, and a and γ are governed by the following modulation equations:

$$a' = -\tfrac{1}{2}\mu a - \frac{F^2\Lambda}{\omega}\sin\gamma \tag{6}$$

$$a\gamma' = -2\sigma a + \frac{S}{\omega}a^3 - \frac{F^2\Lambda}{\omega}\cos\gamma \tag{7}$$

and S is the effective nonlinear coefficient, Λ is the effective forcing coefficient, and μ is the effective damping of the excited mode.

3 RESULTS

We present results describing the superharmonic resonance of order-two of the first mode of the microbeam. The fixed points of equations (6) and (7) are found by setting the time derivatives equal to zero. The stability of the solutions is determined by substituting these solutions into the Jacobian of the equations and examining the numerical values of the eigenvalues for each solution.

We carried out the calculation for a microsensor with the specifications $\alpha_1 = 3.71$, $\alpha_2 = 3.9$, $N = 8.7$, and $Q = 800$. It was found that, as the electrostatic force increases, the effective nonlinearity coefficient decreases monotonically from a *positive* value, crosses zero in the neighborhood of $V_p = 3.27$, continues to decrease, and reaches large *negative* values as the voltage approaches the pull-in voltage. Consequently, the nonlinear behavior of the microbeam changes from a hardening-type at low electrostatic forces to a softening-type at high electrostatic forces. This fact is clearly illustrated in Figures 1 and 2.

The figures show the frequency-response curves for three levels of constant amplitude F. Setting $V_p = 3.1$, in Figure 1, produced $\omega = 22.73$, $S = 38.92$, and $\Lambda = 0.51$. The solid lines in the figure represent stable solutions, while the dashed lines represent unstable solutions. Each curve is composed of three branches: stable lower and upper branches and an unstable branch. Each of the two stable branches meets the unstable branch in a saddle-node bifurcation. The curves are bent to the right, indicating a *hardening-type* nonlinearity and leading to multivalued amplitudes in the region between the two saddle-node bifurcation points. In this region, the response may home on the upper or the lower branch depending on the initial conditions. As σ is decreased very slowly, it reaches the lower saddle-node bifurcation point where the lower branch of solutions disappears and the solution experiences a sudden *jump* up to the upper branch of stable solutions. As σ is increased slowly again, the upper branch disappears at the upper saddle-node bifurcation and the solution jumps down to the lower branch of stable solutions. Both jumps in the response, associated with the forward and backward frequency sweeps, lead to hysteresis.

Setting $V_p = 3.4$, in Figure 2, produced $\omega = 22.19$, $S = -32.42$, and $\Lambda = 0.39$. Figure 2 is similar to Figure 1 except for the fact that the frequency-response curves are bent to the left, indicating a *softening-type* nonlinearity. Also, the frequency-response curve corresponding to $F = 0.3$ does not exhibit any regions of multivalued solutions or unstable solutions.

Figure 3 shows the force-response curve, corresponding to the static loading of Figure 1, for a constant positive detuning $\sigma = 0.05$ (that is; the forcing frequency Ω lies to the right of the natural frequency ω). The

multivalued amplitudes corresponding to the same forcing amplitude F lead to jumps in the response. If F is increased very slowly, the response reaches the lower saddle-node bifurcation D where the response amplitude experiences a sudden *jump* up to the upper branch of stable solutions. Decreasing F at this point decreases the response amplitude till the upper saddle-node bifurcation C where the solution jumps down to the lower branch again. Both jumps in the response, associated with the forward and backward force sweeps, lead to hysteresis.

Figure 4 shows the force-response curve, corresponding to the static loading of Figure 2, for a constant negative detuning $\sigma = -0.05$. The figure is qualitatively similar to Figure 3.

4 CONCLUSIONS

We studied the nonlinear dynamic response of a resonant microsensor under general electric actuation using a nonlinear model of the microbeam valid for moderately large transverse deflections. We used the method of multiple scales to determine the beam response to a superharmonic resonance of order-two and obtained two nonlinear first-order ordinary-differential equations governing the modulation of the amplitude and phase of the response.

Using these equations, we found that the static load V_p has a profound effect on the response of the sensor to a given AC excitation (e.g., a measuring signal). Changes in V_p change the fundamental natural frequency, especially close to the pull-in voltage. More significantly, even when changes in V_p do not lead to significant changes in the fundamental natural frequency, they have a dramatic effect, *qualitatively* and quantitatively, on the frequency-response and force-response curves. As our results show, increasing V_p from 3.1 to 3.4 has a minor effect on the fundamental natural frequency ω, a reduction of 2.4%. On the other hand, it has a drastic effect on the effective nonlinearity coefficient S changing its sign from positive to negative, thus changing the overall system behavior qualitatively from a hardening-type to a softening-type behavior.

The frequency-response and force-response curves show that the microsensor has a region of multivalued solutions and two saddle-node bifurcation points. As a result, sudden jumps in the sensor response and hysteresis are possible. The locations of these bifurcation points and the region of hysteretic behavior depend on the magnitude and sign of the effective nonlinearity coefficient, the effective forcing amplitude, and the damping coefficient.

Finally, the present nonlinear model in conjunction with the perturbation solution provides analytical expressions that present a clear picture of the influence of various design parameters and predict the locations of sudden jumps and regions where multivalued solutions and hysteresis exist, thereby enabling engineers to employ a superharmonic driving signal in resonant microsensors and exploit its superior signal-to-crosstalk ratio as opposed to the first harmonic itself.

REFERENCES

[1] Zook, J. D., Burns, D. W., Guckel, H., Sniegowski, J. J., Engelstad, R. L., and Feng, Z., "Characteristics of polysilicon resonant microbeams," Sensors and Actuators A, Vol. 35, 1992, pp. 290–294.

[2] Gui, C., Legtenberg, R., Tilmans, H. A., Fluitman, J. H., and Elwenspoek, M.,"Nonlinearity and hysteresis of resonant strain gauges," J. Microelectromechanical Systems, Vol. 7, 1998, pp. 122–127.

[3] Tilmans, H. A. and Legtenberg, R., "Electrostatically driven vacuum-encapsulated polysilicon resonators. Part II. Theory and performance," Sensors and Actuators A, Vol. 45, pp. 67–84, 1994.

[4] Turner, G. C. and Andrews, M. K., "Frequency stabilization of electrostatic oscillators," Transducers '95, Stockholm, Sweden, Vol. 2, pp. 624–626, 1995.

[5] Ayela, F. and Fournier, T., "An experimental study of anharmonic micromachined silicon resonators," Measurement, Science and Technology, Vol. 9, pp. 1821–1830, 1998.

[6] Veijola, T., Mattila, T., Jaakkola, O., Kiihamäki, J., Lamminmäki, T., Oja, A., Ruokonen, K., Sepä, H., Seppälä, P., and Tittonen, I., "Large-displacement modelling and simulation of micromechanical electrostatically driven resonators using the harmonic balance method," IEEE MTT-S, Vol. 1, pp. 99–102, 2000.

[7] Jin, Z. and Wang, Y., "Electrostatic resonator with second superharmonic resonance," Sensors and Actuators A, Vol. 64, pp. 273–279, 1998.

[8] Abdel-Rahman, E. M., Younis, M. I., and Nayfeh, A. H., "Characterization of the mechanical behavior of an electrically actuated microbeam," J. Micromech. Microeng., Vol. 12, pp. 759–766, 2002.

[9] Younis, M. I. and Nayfeh, A. H., "A study of the nonlinear response of a microbeam to an electric actuation," to appear in Nonlinear Dynamics.

[10] Nayfeh, A. H., *Introduction to Perturbation Techniques,* Wiley, New York, 1981.

[11] Nayfeh, A. H. and Mook, D. T., *Nonlinear Oscillations,* Wiley, New York, 1979.

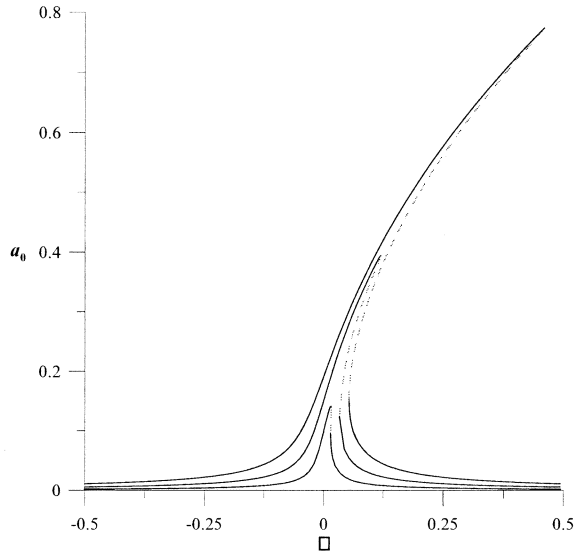

Figure 1: Frequency-response curves for $F = 0.3, 0.5,$ and 0.7 and $V_p = 3.1$.

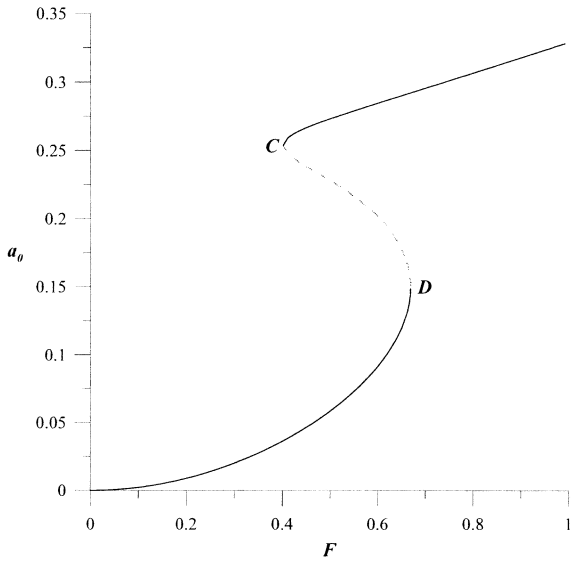

Figure 3: Force-response curve for $\sigma = 0.05$ and $V_p = 3.1$.

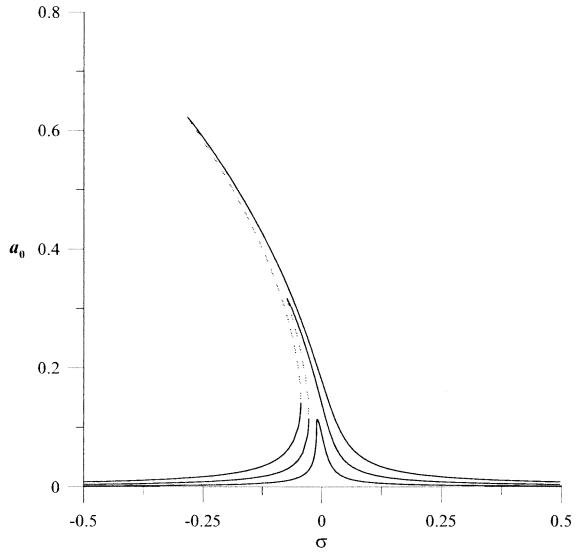

Figure 2: Frequency-response curves for $F = 0.3, 0.5,$ and 0.7 and $V_p = 3.4$.

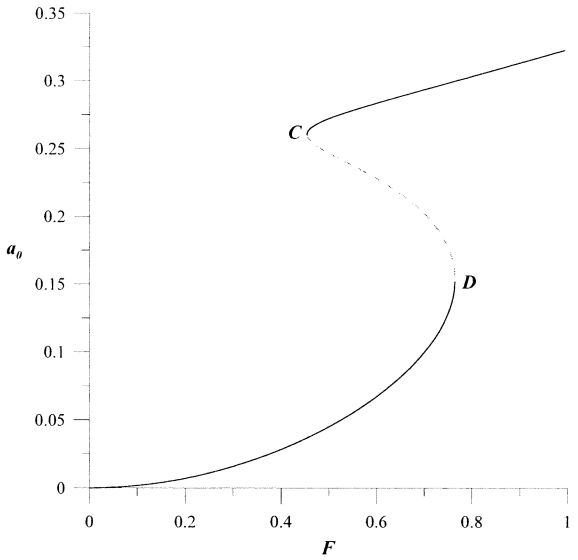

Figure 4: Force-response curve for $\sigma = -0.05$ and $V_p = 3.4$.